

Micro-Raman investigation of aligned single-wall carbon nanotubes

C. Fantini,¹ M. A. Pimenta,^{1,*} M. S. S. Dantas,¹ D. Ugarte,² A. M. Rao,³ A. Jorio,⁴ G. Dresselhaus,⁵ and M. S. Dresselhaus^{4,6}

¹*Departamento de Física, Universidade Federal de Minas Gerais, Caixa Postal 702, 30123-970 Belo Horizonte, Brazil*

²*Laboratório Nacional de Luz Síncrotron, Caixa Postal 6192, 13083-970 Campinas, Brazil*

³*Department of Physics and Astronomy, Clemson University, Clemson, South Carolina 29634-0978*

⁴*Department of Physics, Massachusetts Institute of Technology, Cambridge, Massachusetts 02139-4307*

⁵*Francis Bitter Magnet Laboratory, Massachusetts Institute of Technology, Cambridge, Massachusetts 02139-4307*

⁶*Department of Electrical Engineering and Computer Science, Massachusetts Institute of Technology, Cambridge, Massachusetts 02139-4307*

(Received 22 December 2000; revised manuscript received 15 February 2001; published 6 April 2001)

Polarized micro-Raman experiments were performed on samples of aligned single-wall carbon nanotubes (SWNTs) previously characterized by scanning electron microscopy. The analysis of the different spectral shapes of the tangential G band, when the position of the laser beam changes from spot to spot on the sample, allows us to distinguish the contribution from *metallic* and *semiconducting* nanotubes. The angular dependence of the polarized spectra reveals that the line around $\sim 1580\text{ cm}^{-1}$ is an intrinsic feature of *metallic* SWNTs. Moreover, it is shown that the “antenna” effect for the Raman scattering in SWNTs is stronger for metallic than for semiconducting nanotubes.

DOI: 10.1103/PhysRevB.63.161405

PACS number(s): 78.30.Na, 78.66.Tr

I. INTRODUCTION

Polarized Raman spectroscopy is a useful tool studying the symmetry of the vibrational modes of carbon nanotubes.¹⁻⁴ Considering only the tangential modes, which originate from the E_{2g_2} phonon mode of graphite, group theory predicts six Raman-active modes for a single-wall nanotube (SWNT): two A , two E_1 , and two E_2 symmetry modes for chiral nanotubes and only three (A_{1g} , E_{1g} , E_{2g}) for the symmorphic armchair and zig-zag SWNTs).^{1,5} The A (A_{1g}) modes are expected to appear in the ZZ and XX polarized Raman spectra (the Z direction is along the nanotube axis), while the E_1 (E_{1g}) modes can be present in crossed-polarized configurations (XZ and ZX configurations), and the E_2 (E_{2g}) modes are expected to appear only in the XX configuration (incident and scattered polarizations perpendicular to the nanotube axis).

In a recent polarized Raman study of aligned bundles of SWNTs (Ref. 6) using 2.41 eV laser excitation energy, it was shown that the tangential band exhibits four distinct peaks intrinsically associated with *semiconducting* SWNTs. Two weak peaks around $\sim 1550\text{ cm}^{-1}$ and $\sim 1610\text{ cm}^{-1}$ only appear in the XX configuration and, therefore, they are associated with the E_2 (E_{2g}) symmetry modes. Two other peaks (around $\sim 1565\text{ cm}^{-1}$ and $\sim 1590\text{ cm}^{-1}$) correspond to unresolved modes with A (A_{1g}) and E_1 (E_{1g}) symmetries, since the two features appear in all polarization configurations, including the XX configuration. Also shown in this study was the presence of a fifth peak around 1580 cm^{-1} , whose intensity was strongly dependent on the position of the laser spot on the sample, but its origin was not well understood.

Recently, Duesberg *et al.*⁷ reported a polarized Raman study of isolated nanotubes using 1.96 eV laser excitation energy, where it was shown that the intensity of all Raman bands vanishes when the polarization of the incident and scattered beams are perpendicular to the nanotube axis (XX

spectrum). In particular, it was observed that the intensity of the tangential band depends on $\cos^2\theta$, where θ is the angle between the nanotube axis and the light polarization direction. This result was attributed to the depolarization effect (“antenna” effect) proposed by Ajiki and Ando⁸ according to which the interband optical transitions from the valence band to the conducting band near the Fermi level can be observed only for polarization parallel to the tube axis.

In order to understand the apparent discrepancies between these two studies,^{6,7} we performed a polarized micro-Raman study of aligned SWNT bundles using 1.92 eV laser excitation. We introduce a methodology in the analysis of the experimental data which subtracts the spectra from large diameter SWNTs and multi-wall nanotubes (MWNTs), allowing us to analyze only the contribution from isolated small diameter SWNTs. We show that it is possible to obtain the spectra from *metallic* and *semiconducting* nanotubes separately by changing the position of the laser spot on the sample. The angular dependence of the polarized spectra associated with these two different types of nanotubes reveals that the “antenna” effect is stronger for the *metallic* SWNTs. Moreover, it is shown that the narrow peak around 1580 cm^{-1} is an intrinsic feature of *metallic* carbon nanotubes.

II. EXPERIMENTAL DETAILS

Aligned SWNTs were prepared using a hydrogen and argon electric arc method as described in Ref. 9. The sample is composed of a few bundles of SWNTs having very good tube alignment, and the sample exhibits a broad distribution of tube diameters, centered at $d_t = 1.85\text{ nm}$ ($\Delta d = 0.25\text{ nm}$). However, the sample is inhomogeneous as far as the tube diameter distribution is concerned, and smaller tubes down to 1.3 nm can also be found in local areas of the sample. In order to check the alignment of the bundles, the sample was investigated by scanning electron microscopy (SEM) (JSM-6330F, LME/LNLS, Campinas, Brazil). The SWNT bundles were dispersed on TEM indexed copper grids in such a way

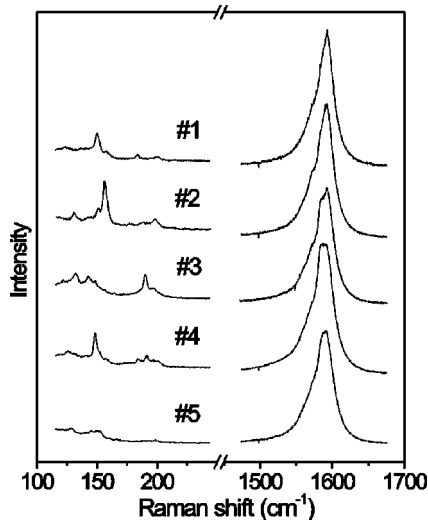


FIG. 1. Raman spectra recorded with the 1.92 eV laser excitation line at five different spots on the sample.

that the coordinates of the bundles could be determined in the SEM and subsequently located again with the micro-Raman instrument.

Back-scattering micro-Raman experiments were performed at room temperature, using a triple monochromator micro-Raman spectrometer (DILOR XY) and the Kr-laser excitation line at 647.1 nm (1.92 eV). A 100 \times microscope objective was used for focusing the laser beam on the sample and for collecting the scattered light. The laser spot has a diameter of $\sim 1 \mu\text{m}$ at the sample and the power density was $\approx 10^4 \text{ W/cm}^2$. In the polarized Raman experiments, half-wave plates were inserted before and after the sample, allowing the rotation of the incident and scattered polarizations. The spectra were recorded using the VV configuration (same polarization for the incident and scattered light), by changing the angle between the nanotube axis and the polarization direction.

III. RESULTS AND DISCUSSION

Figure 1 shows the micro-Raman spectra recorded at five different spots on the aligned sample, displaced from each other by a few microns, using the ZZ scattering geometry. Note that the radial breathing mode (RBM) band, between 100 and 200 cm^{-1} , is strongly dependent on the laser spot position. We can observe in spectrum No. 5 only the presence of a broad RBM band centered at low frequency. In fact this is a typical shape of the RBM found in different spots of the sample, and it reflects the broad diameter distribution of SWNTs measured by high-resolution (HR) TEM ($d_t = 1.85 \pm \Delta d_t$, $\Delta d_t = 0.25 \text{ nm}$). However, in some local areas we can also detect small diameter SWNTs. For example, in spectra No. 1 to No. 4 we can also observe the presence of different sharp RBM peaks, superimposed to the broad band observed in spectrum No. 5. These peaks reveal that, besides the broad distribution of large diameter tubes, some small diameter tubes can also be found in these areas of the sample.

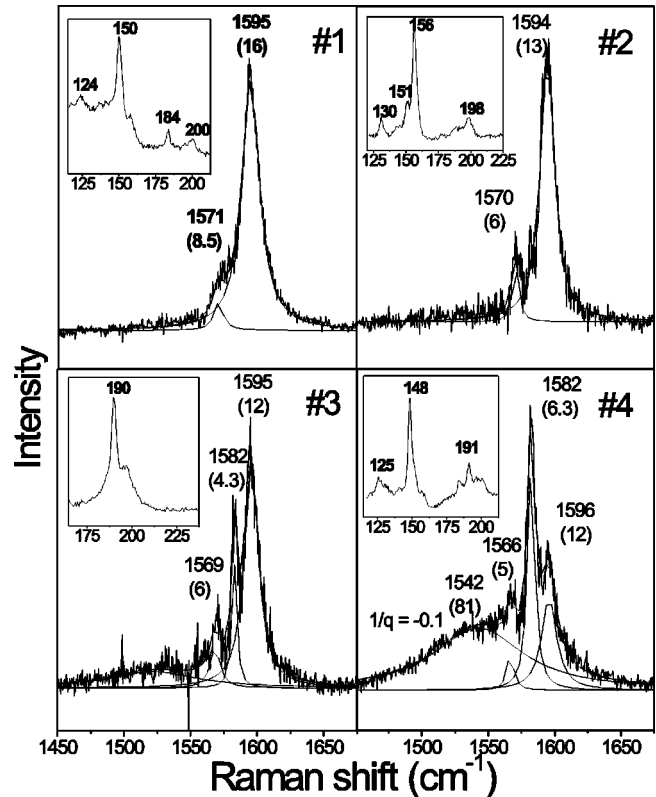


FIG. 2. Lorentzian line-shape analysis for the subtracted spectra. The frequencies and linewidths (in brackets) of observed tangential G-band modes are also displayed. The RBM spectra are shown in the insets.

In order to study only the contribution from small diameter SWNTs for the Raman spectra, spectrum No. 5 shown in Fig. 1 has been subtracted from spectra No. 1 to No. 4. Figure 2 shows the subtracted spectra associated with regions No. 1 to No. 4. The scaling in the subtraction procedure was done such that the subtracted spectra in the RBM region (insets of Fig. 2) shows only the sharp peaks, thus eliminating the broad RBM band associated with large diameter nanotubes.

Note that the tangential band of the subtracted spectra No. 1 and No. 2 can be fitted using only two Lorentzian peaks around 1570 and 1594 cm^{-1} . In fact, these are typical ZZ spectra of aligned *semiconducting* SWNTs, in which the E_2 (E_{2g}) modes are not expected to appear.⁶ The subtracted spectrum No. 4 is quite different from the subtracted spectra No. 1 and No. 2. We can observe in this case two weak peaks typical of *semiconducting* nanotubes (at 1566 and 1596 cm^{-1}), but the spectrum is dominated by a broad feature around 1542 cm^{-1} and a sharp peak at 1582 cm^{-1} . Spectrum No. 3 corresponds to an intermediate situation between spectra No. 1 and No. 2 and spectrum No. 4.

In a previous resonant Raman study of SWNTs,¹⁰ it was shown that the tangential band for *metallic* nanotubes exhibits a broad feature around 1540 cm^{-1} and a narrow peak around 1580 cm^{-1} , when the incident or scattered photons are in resonance with the optical transition E_{11}^M for *metallic* tubes. Moreover, the broad feature around 1540 cm^{-1} has a

Breit–Wigner–Fano (BWF) line shape,¹¹ which is related to the coupling between phonons and a continuum of electronic states.

The broad feature in spectra No. 3 and No. 4 in Fig. 2 has been fit using a BWF curve given by

$$I(\omega) = I_0 \frac{[1 + (\omega - \omega_{\text{BWF}})/q\Gamma]^2}{[1 + [(\omega - \omega_{\text{BWF}})/\Gamma]^2]}, \quad (1)$$

where $1/q$ is a measure of the interaction between phonons and a continuum of electronic states, ω_{BWF} is the BWF peak frequency at maximum intensity I_0 , and Γ is the half width of the BWF peak.¹¹ The fit parameters of these BWF lines are $\omega_{\text{BWF}} = 1540 \text{ cm}^{-1}$, $1/q = -0.1$, and $\Gamma = 87 \text{ cm}^{-1}$. The line at 1582 cm^{-1} is fit by a Lorentzian curve and it appears associated with the downshifted BWF line.

The insets of Fig. 2 show the corresponding subtracted spectra in the spectral region of the radial breathing modes of the nanotubes. Using the recently proposed expression which relates the RBM frequency ω_{RBM} and the nanotube diameter d_t for isolated nanotubes¹² ($\omega_{\text{RBM}} = 248 \text{ cm}^{-1} \text{ nm}/d_t$), the RBM peaks were expected to appear between 120 and 155 cm^{-1} , since the mean diameter of the SWNTs present in the sample is $d_t = 1.85 \pm 0.25 \text{ nm}$. A broad and asymmetric RBM band can be observed in spectrum No. 5 of Fig. 1, and this band is associated with a distribution of large diameter SWNTs, which are predominant in the sample. The fact that this broad band is weak, compared to the relatively higher frequency sharp peaks observed in spectra No. 1 to No. 4, is due to the decrease of the Raman cross section for RBM modes with increasing diameter. The sharp RBM peaks observed in spectra No. 1 to No. 4 have frequencies between 150 and 190 cm^{-1} and, therefore, are associated with SWNTs having diameters in the range 1.3–1.65 nm. The presence of peaks in this frequency range is in agreement with HRTEM measurements,⁹ in which small diameter SWNTs were also found in the sample.

Considering all SWNTs in the diameter range 1.3–2.1 nm, we expect in a Raman Stokes experiment with $E_{\text{laser}} = 1.92 \text{ eV}$ the observation of the spectra for *metallic* SWNTs when the incident or the scattered photons are in resonance with the E_{11}^M optical transition, and the spectra for *semiconducting* SWNTs when the resonance occurs with the E_{33}^S transition.^{1,5} Taking into account the diameter dependence of the energy separations E_{ii} ,¹ the *metallic* nanotubes observed in our resonance Raman experiment are expected to have diameters in the range 1.3–1.4 nm and the *semiconducting* SWNTs to have diameters in the range 1.5–1.9 nm. Therefore with $E_{\text{laser}} = 1.92 \text{ eV}$, the sharp RBM peaks observed in Fig. 1 around 150 cm^{-1} are associated with *semiconducting* SWNTs, whereas those around 190 cm^{-1} are associated with *metallic* nanotubes. Note in the inset of the subtracted spectrum No. 4 (Fig. 2) that the *semiconducting* RBM peak at 148 cm^{-1} is more intense than the *metallic* RBM peaks around 190 cm^{-1} , whereas the tangential mode (TM) band is dominated by the *metallic* modes (1540 and 1582 cm^{-1}). This result can be explained in terms of the different energy ranges for the resonant processes of the scattered photons associated with the RBM and TM bands.¹

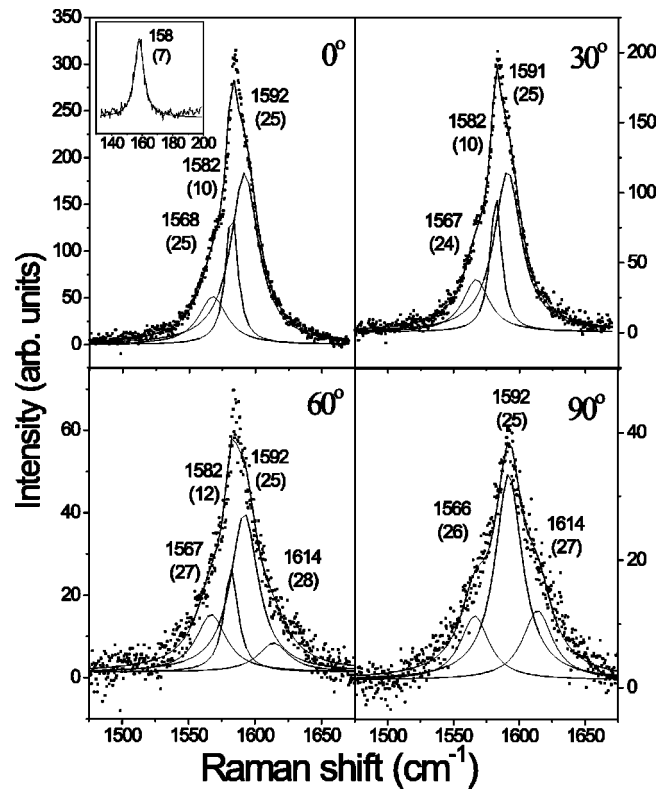


FIG. 3. Angular dependence of the VV polarized tangential mode spectra recorded with 1.92 eV laser excitation. The frequencies and linewidths (in parentheses) of observed modes are also displayed.

It is worth mentioning that all graphitic sp^2 materials exhibit a Raman peak around 1580 cm^{-1} . In order to confirm that the peak around 1582 cm^{-1} is an intrinsic feature of SWNTs, we have performed polarized micro-Raman measurements by changing the angle θ between the nanotube axis and the light polarization direction. The VV spectra for $\theta = 0^\circ$ corresponds to the ZZ configuration, and $\theta = 90^\circ$ corresponds to the XX configuration. Figure 3 shows the angular dependence of the tangential band in the VV spectra. In the $\theta = 0^\circ$ spectrum (ZZ polarization), we can observe two peaks at 1567 and 1592 cm^{-1} , which are associated with *semiconducting* SWNTs, and a third peak around 1582 cm^{-1} . The BWF feature in this case is very weak and is not observed. Note that the intensity of the whole tangential band decreases with increasing θ but only the peak at 1582 cm^{-1} vanishes for $\theta = 90^\circ$. On the other hand, a new peak around 1614 cm^{-1} is observed in the $\theta = 60^\circ$ and $\theta = 90^\circ$ spectra. This peak is associated with an E_2 (E_{2g}) mode, which is expected to appear in the XX spectrum.⁶ The appearance of this E_2 (E_{2g}) mode in the XX spectrum confirms the alignment of the SWNTs in the sample.

In a recent polarized Raman study of isolated SWNTs, Duesberg *et al.*⁷ showed that the intensity of the Raman modes is proportional to $\cos^2 \theta$, and that all bands vanish in the XX configuration. This work was performed with the 1.96 eV laser excitation energy, and the tangential band has a line shape typical of *metallic* tubes.¹⁰ On the other hand, Jorio *et al.*⁶ showed that the tangential band of *semiconduct-*

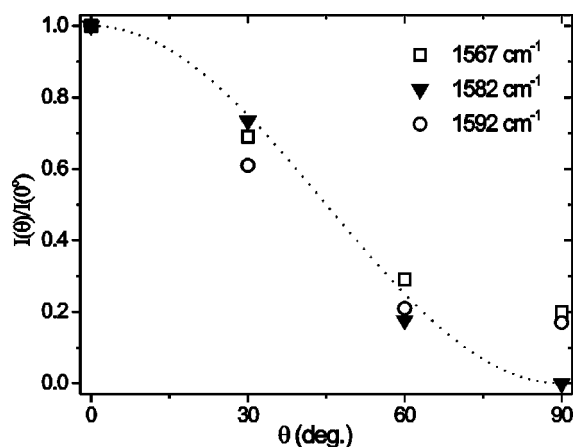


FIG. 4. Angular dependence of the relative intensities of the peaks around 1567, 1582, and 1592 cm^{-1} normalized to their intensities for $\theta=0^\circ$. The dotted curve corresponds to the function $\cos^2 \theta$.

ing SWNTs, investigated with the 2.41 eV laser energy, does not vanish in the XX spectrum. In particular, the intensities of the peaks around 1567 and 1590 cm^{-1} in the XX spectrum for semiconducting SWNTs drop by a factor of 4 with respect to their intensities in the ZZ spectrum.

Figure 4 shows the angular dependence of the relative intensities of the peaks around 1567, 1582, and 1592 cm^{-1} normalized to their intensities for $\theta=0^\circ$. Note that the intensity of the peak at 1582 cm^{-1} varies with $\cos^2 \theta$ (dotted curve in Fig. 4), in agreement with the results reported in Ref. 7. This result can be explained in terms of the “antenna” effect due to the strong anisotropic geometry of the nanotubes, which the present work shows is very important for metallic nanotubes and appears to be less important for semiconducting nanotubes. On the other hand, the intensities of the peaks at 1567 and 1592 cm^{-1} , associated with *semiconducting* nanotubes, both decrease with increasing θ (see Fig. 4), but both of these features are still present in the XX spectrum ($\theta=90^\circ$).

All experimental results discussed above lead us to conclude that the Raman peak around 1582 cm^{-1} is intrinsically associated with *metallic* SWNTs and that the “antenna” effect, observed in the polarized Raman studies of aligned SWNTs, is stronger for *metallic* than for *semiconducting* nanotubes, due to the finite value of the electronic density of states at the Fermi level for metallic SWNTs.

IV. CONCLUSION

In this work, a polarized micro-Raman study of bundles of SWNTs is presented, showing good nanoscale alignment. The experiments were performed in marked regions of the sample, previously investigated by SEM. The majority of the nanotubes in the sample exhibit diameters in the range $d_t = 1.85 \pm 0.25$ nm, giving rise to a broad RBM band below 150 cm^{-1} . However, very sharp Raman peaks are sometimes found superimposed on the broad RBM band, indicating also the presence of some small diameter SWNTs in the sample.

The frequencies of the sharp RBM peaks, and the shape of the associated tangential bands, depend strongly on the position of the laser spot on the sample, thus allowing the observation of the Raman spectra from *metallic* or *semiconducting* SWNTs to be disentangled from each other. The angular dependence of the tangential peak at 1582 cm^{-1} , whose intensity in the VV spectra varies as $\cos^2 \theta$, suggests that this feature is intrinsically associated with *metallic* SWNTs. Moreover, our results show that the “antenna” effect in the polarized Raman spectra of aligned SWNTs is stronger for the *metallic* nanotubes.⁶

We thank Professor H.M. Cheng of the Institute for Metals in Shenyang, China for providing us with the sample and Paulo C. Silva for performing the SEM experiments. We acknowledge the NSF/CNPq joint collaboration program that makes possible exchange trips between MIT and UFMG researchers (NSF Grant No. INT.00-00408 and CNPq Grant No. 910120/99-4). The MIT authors acknowledge support under NSF Grant No. DMR 98-04734. A.M.R acknowledges support from NSF MRSEC while at the University of Kentucky.

*Corresponding author. Email address: mpimenta@fisica.ufmg.br
¹M. S. Dresselhaus and P. C. Eklund, *Adv. Phys.* **49**, 705 (2000).
²H. D. Sun, Z. K. Tang, J. Chen, and G. Li, *Solid State Commun.* **109**, 365 (1999).
³C. Thomsen, S. Reich, P. M. Rafailov, and H. Jantoljak, *Phys. Status Solidi B* **214**, R15 (1999).
⁴A. M. Rao, A. Jorio, M. A. Pimenta, M. S. S. Dantas, R. Saito, G. Dresselhaus, and M. S. Dresselhaus, *Phys. Rev. Lett.* **84**, 1820 (2000).
⁵R. Saito, G. Dresselhaus, and M. S. Dresselhaus, *Physical Properties of Carbon Nanotubes* (Imperial College Press, London, 1988).
⁶A. Jorio, G. Dresselhaus, M. S. Dresselhaus, M. Souza, M. S. S. Dantas, M. A. Pimenta, A. M. Rao, C. Liu, and H. M. Cheng, *Phys. Rev. Lett.* **85**, 2617 (2000).

⁷G. S. Duesberg, I. Loa, M. Burghard, K. Syassen, and S. Roth, *Phys. Rev. Lett.* **85**, 5436 (2000).
⁸H. Ajiki and T. Ando, *Physica B* **201**, 349 (1994).
⁹C. Liu, H. T. Cong, F. Li, P. H. Tan, H. M. Cheng, K. Lu, and B. L. Zhou, *Carbon* **37**, 1865 (1999).
¹⁰M. A. Pimenta, A. Marucci, S. Empedocles, M. Bawendi, E. B. Hanlon, A. M. Rao, P. C. Eklund, R. E. Smalley, G. Dresselhaus, and M. S. Dresselhaus, *Phys. Rev. B* **58**, R16 016 (1998).
¹¹S. D. M. Brown, A. Jorio, P. Corio, M. S. Dresselhaus, G. Dresselhaus, R. Saito, K. Kneipp, *Phys. Rev. B* (to be published).
¹²A. Jorio, R. Saito, J. H. Hafner, C. M. Lieber, M. Hunter, T. McClure, G. Dresselhaus, and M. S. Dresselhaus, *Phys. Rev. Lett.* **86**, 1118 (2001).